*Hin*dIII/*Bgl*II-digested pRS in 96-well plates. Ligation reactions were transformed into competent DH5α bacteria. Bacterial cultures were grown overnight and plasmid DNA was isolated. All manipulations were performed using a Multimek robot.

Additional information about the NKi RNAi library can be found at http://screeninc.nki.nl/.

### Cell culture, transfection and retroviral infection

BJ fibroblasts were cultured in a 4:1 mixture of DMEM:M199 supplemented with 15% heat-inactivated fetal calf serum. U2-OS and Phoenix cells were cultured in DMEM supplemented with 10% heat-inactivated fetal calf serum. Transfections were performed with the calcium phosphate precipitation technique. Ecotropic retroviral supernatants were produced by transfection of Phoenix packaging cells. Viral supernatants were filtered through a 0.45 μm filter, and infections were performed in the presence of 4 $\mu g\,ml^{-1}$ polybrene (Sigma). Drug selections in U2-OS cells were performed with 2 $\mu g\,ml^{-1}$ puromycin and 200 $\mu g\,ml^{-1}$ zeocin (Invitrogen).

### Recovery of shRNA inserts

Genomic DNA was isolated from expanded colonies using DNAzol (Life Technologies). PCR amplification of the shRNA inserts was performed with Expand Long Template PCR system (Roche) and the use of pRS-fw primer: 5′-CCCTTGAACCTCCTCGTTCGACC-3′ and pRS-rev primer: 5′-GAGACGTGCTACTTCCATTTGTC-3′. Products were digested with *Eco*RI/*Xho*I and recloned into pRS. Hairpins were sequenced with Big Dye Terminator (Perkin Elmer) using pRS-seq primer: 5′-GCTGACGTCATCAACCCGCT-3′.

### Cell-cycle analysis

For fluorescence-activated cell sorting (FACS) analysis, U2-OS cells were co-transfected with H2B–GFP to select for transfected cells. Forty-eight hours after transfection, cells were treated with IR (5 or 10 Gy). Twenty-four hours after IR, the cells were washed and fixed in 70% ethanol at 4 °C. Before FACS analysis, cells were washed with PHN (PBS, 20 mM HEPES, 0.5% NP40) and incubated with 10 $\mu g\,ml^{-1}$ propidium iodide and 250 $\mu g\,ml^{-1}$ RNase A. In each assay, 8,000 GFP-positive cells were collected by FACScan and analysed using the CellQuest program (Becton Dickinson).

### Western and northern blotting

For western blots, puromycin-selected cells were lysed in RIPA buffer (50 mM Tris pH 8; 150 mM NaCl; 1% NP40; 0.5% DOC; 0.1% SDS). Thirty micrograms of protein was separated on 8–12% SDS–polyacrylamide gel electrophoresis and transferred to polyvinylidine difluoride membranes (Millipore). Western blots were probed with antibodies. For northern analysis, 15 μg total RNA was loaded on a 1% agarose gel and blotted onto Hybond N+ (Amersham). $^{32}$P-labelled probes for p21 and BAX were generated with PCR labelling.

### siRNA bar-code screens

The shRNA inserts were amplified from genomic DNA by PCR using the primers pRS-fw primer 5′-CCCTTGAACCTCCTCGTTCGACC-3′ and pRS8-rev primer 5′-TAAAGCGCATGCTCCAGACT-3′. PCR products were labelled with cyanine-3 or cyanine-5 fluorescent groups using the Universal Linkage System (ULS; Kreatech Biotechnology) and purified over a KreaPure (Kreatech Biotechnology) spin column as described previously[28]. PCR products from two samples were combined and hybridized to oligonucleotide arrays in 40 μl of 25% formamide, 5×SCC, 0.01% SDS (containing poly d(A), yeast transfer RNA and COT-1 DNA). Samples were heated to 100 °C for 1 min and applied to the array. Samples were hybridized for 18 h at 42 °C, washed and scanned using an Agilent microarray scanner. Quantification of the resulting fluorescent images was performed with Imagene 5.6 (BioDiscovery); the local background was subtracted and the data normalized and $^{2}$log transformed. Additional information on bar-code screens can be found at http://screeninc.nki.nl/.

Received 11 November 2003; accepted 26 January 2004; doi:10.1038/nature02371.


1. Lum, L. *et al.* Identification of Hedgehog pathway components by RNAi in *Drosophila* cultured cells. *Science* **299,** 2039–2045 (2003).
2. Kamath, R. S. *et al.* Systematic functional analysis of the *Caenorhabditis elegans* genome using RNAi. *Nature* **421,** 231–237 (2003).
3. Ashrafi, K. *et al.* Genome-wide RNAi analysis of *Caenorhabditis elegans* fat regulatory genes. *Nature* **421,** 268–272 (2003).
4. Brummelkamp, T. R., Bernards, R. & Agami, R. A system for stable expression of short interfering RNAs in mammalian cells. *Science* **296,** 550–553 (2002).
5. Paddison, P. J., Caudy, A. A., Bernstein, E., Hannon, G. J. & Conklin, D. S. Short hairpin RNAs (shRNAs) induce sequence-specific silencing in mammalian cells. *Genes Dev.* **16,** 948–958 (2002).
6. Hannon, G. J. RNA interference. *Nature* **418,** 244–251 (2002).
7. Elbashir, S. M. *et al.* Duplexes of 21-nucleotide RNAs mediate RNA interference in cultured mammalian cells. *Nature* **411,** 494–498 (2001).
8. Sherr, C. J. The ink4a/ARF network in tumour suppression. *Nature Rev. Mol. Cell Biol.* **2,** 731–737 (2001).
9. Brummelkamp, T., Bernards, R. & Agami, R. Stable suppression of tumorigenicity by virus-mediated RNA interference. *Cancer Cell* **2,** 243–247 (2002).
10. Brummelkamp, T. R., Nijman, S. M., Dirac, A. M. & Bernards, R. Loss of the cylindromatosis tumour suppressor inhibits apoptosis by activating NF-κB. *Nature* **424,** 797–801 (2003).
11. Semizarov, D. *et al.* Specificity of short interfering RNA determined through gene expression signatures. *Proc. Natl Acad. Sci. USA* **100,** 6347–6352 (2003).
12. Jackson, A. L. *et al.* Expression profiling reveals off-target gene regulation by RNAi. *Nature Biotechnol.* **21,** 635–637 (2003).
13. Kamijo, T. *et al.* Tumor suppression at the mouse INK4a locus mediated by the alternative reading frame product p19ARF. *Cell* **91,** 649–659 (1997).
14. Lakin, N. D. & Jackson, S. P. Regulation of p53 in response to DNA damage. *Oncogene* **18,** 7644–7655 (1999).
15. El-Deiry, W. S. *et al.* WAF1, a potential mediator of p53 tumor suppression. *Cell* **75,** 817–825 (1993).
16. Brugarolas, J. *et al.* Radiation-induced cell cycle arrest compromised by p21 deficiency. *Nature* **377,** 552–557 (1995).
17. Waldman, T., Kinzler, K. W. & Vogelstein, B. p21 is necessary for the p53-mediated G1 arrest in human cancer cells. *Cancer Res.* **55,** 5187–5190 (1995).
18. Brown, J. P., Wei, W. & Sedivy, J. M. Bypass of senescence after disruption of p21CIP1/WAF1 gene in normal diploid human fibroblasts. *Science* **277,** 831–834 (1997).
19. Miyashita, T. & Reed, J. C. Tumor suppressor p53 is a direct transcriptional activator of the human bax gene. *Cell* **80,** 293–299 (1995).
20. Barak, Y., Juven, T., Haffner, R. & Oren, M. mdm2 expression is induced by wild type p53 activity. *EMBO J.* **12,** 461–468 (1993).
21. Kubbutat, M. H., Jones, S. N. & Vousden, K. H. Regulation of p53 stability by Mdm2. *Nature* **387,** 299–303 (1997).
22. Brummelkamp, T. R. & Bernards, R. New tools for functional mammalian cancer genetics. *Nature Rev. Cancer* **3,** 781–789 (2003).
23. Shoemaker, D. D., Lashkari, D. A., Morris, D., Mittmann, M. & Davis, R. W. Quantitative phenotypic analysis of yeast deletion mutants using a highly parallel molecular bar-coding strategy. *Nature Genet.* **14,** 450–456 (1996).
24. Brummelkamp, T. R. *et al.* TBX-3, the gene mutated in Ulnar-Mammary Syndrome, is a negative regulator of p19ARF and inhibits senescence. *J. Biol. Chem.* **277,** 6567–6572 (2002).
25. Kanda, T., Sullivan, K. F. & Wahl, G. M. Histone–GFP fusion protein enables sensitive analysis of chromosome dynamics in living mammalian cells. *Curr. Biol.* **8,** 377–385 (1998).
26. Wang, A. H. *et al.* HDAC4, a human histone deacetylase related to yeast HDA1, is a transcriptional corepressor. *Mol. Cell. Biol.* **19,** 7816–7827 (1999).
27. Schwarz, D. S. *et al.* Asymmetry in the assembly of the RNAi enzyme complex. *Cell* **115,** 199–208 (2003).
28. Heetebrij, R. J. *et al.* Platinum(II)-based coordination compounds as nucleic acid labeling reagents: synthesis, reactivity, and applications in hybridization assays. *Chembiochem* **4,** 573–583 (2003).
29. Trettel, F. *et al.* Dominant phenotypes produced by the HD mutation in STHdh(Q111) striatal cells. *Hum. Mol. Genet.* **9,** 2799–2809 (2000).
30. Dirac, A. M. & Bernards, R. Reversal of senescence in mouse fibroblasts through lentiviral suppression of p53. *J. Biol. Chem.* **278,** 11731–11734 (2003).


**Supplementary Information** accompanies the paper on **www.nature.com/nature**.

**Acknowledgements** We thank S. Friend and J. Downward for their support of this project, M. Voorhoeve, Z. Wu, X.-j. Yang, H. Yntema and Kreatech Biotechnology for reagents, the NKI microarray facility group for assistance, A. Dirac and S. Nijman for technical help, and members of the Bernards laboratory for discussions. This work was supported by grants from the Netherlands Genomics Initiative/Netherlands Organization for Scientific Research (NWO), Cancer Research UK (CRUK), the Centre for Biomedical Genetics (CBG), the Dutch Cancer Society (KWF) and Utrecht University (ABC cluster).

**Competing interests statement** The authors declare that they have no competing financial interests.

**Correspondence** and requests for materials should be addressed to R.L.B. (r.beijersbergen@nki.nl) or R.B. (r.bernards@nki.nl).

# Functional interactions between receptors in bacterial chemotaxis

**Victor Sourjik*** **& Howard C. Berg**

[1]*Department of Molecular and Cellular Biology, Harvard University, 16 Divinity Avenue, Cambridge, Massachusetts 02138, and the Rowland Institute at Harvard, 100 Edwin H. Land Boulevard, Cambridge, Massachusetts 02142, USA*

* Present address: ZMBH, University of Heidelberg, Im Neuenheimer Feld 282, D-69120, Germany

**Bacterial chemotaxis is a model system for signal transduction, noted for its relative simplicity, high sensitivity, wide dynamic range and robustness. Changes in ligand concentrations are sensed by a protein assembly consisting of transmembrane receptors, a coupling protein (CheW) and a histidine kinase (CheA)[1–4]. In *Escherichia coli*, these components are organized at the cell poles in tight clusters that contain several thousand copies of each protein[1,4–6]. Here we studied the effects of variation**

**in the composition of clusters on the activity of the kinase and its sensitivity to attractant stimuli, monitoring responses *in vivo* using fluorescence resonance energy transfer. Our results indicate that assemblies of bacterial chemoreceptors work in a highly cooperative manner, mimicking the behaviour of allosteric proteins. Conditions that favour steep responses to attractants in mutants with homogeneous receptor populations also enhance the sensitivity of the response in wild-type cells. This is consistent with a number of models[7–11] that assume long-range cooperative interactions between receptors as a general mechanism for signal integration and amplification.**

The regulation of the autokinase activity of CheA has been described in terms of a two-state model in which a receptor is in either an active or an inactive state, either promoting or inhibiting the activity of CheA[12–15]. Binding of attractant increases the probability that a receptor is inactive, whereas methylation of a receptor on four specific glutamate residues increases the probability that it is active[3,4,16]. Receptors in lower modification states, although less active, have higher affinities to attractant[15–18]. In its simple form, the two-state model is unable to explain many features of the chemotactic response, such as high sensitivity and integration of different stimuli. *Escherichia coli* has five types of receptor: two high-abundance receptors, for aspartate (Tar) and serine (Tsr), and three low-abundance receptors, Tap, Trg and Aer. There is growing evidence of interactions between receptors in the cell[19,20], and modifications of the two-state model have been proposed to account for signal amplification and integration based on receptor–receptor interactions that induce long-range cooperative behaviour[7–11]. *In vitro* studies of receptor cooperativity have shown both high[18] and low[21,17] cooperativity. Here we explore interactions between receptors *in vivo*.

We used an assay based on fluorescence resonance energy transfer (FRET) to monitor the activity of the kinase CheA in a cell population. This assay relies on phosphorylation-dependent interactions of the response regulator CheY, fused to yellow fluorescent protein (YFP), with its phosphatase CheZ, fused to cyan fluorescent protein (CFP). Under the conditions of our experiment, CheY is phosphorylated by CheA at the same rate at which CheY-P is dephosphorylated by CheZ, so the kinase activity can be inferred from the concentration of the CheZ–CheY-P enzyme–substrate complex and expressed in units of FRET; that is, as a function of the degree to which excitation of CFP generates fluorescence of YFP[22]. We added and subtracted attractant over a range of concentrations and constructed dose–response curves that, for convenience, were fit by the Hill equation, yielding a sensitivity, $K_{1/2}^{-1}$, characterized by the ligand concentration at half-maximal response, $K_{1/2}$, and a cooperativity characterized by the Hill coefficient, $H$ (see Supplementary Information). These experiments were repeated with cells in which the levels of expression of Tar, Tsr, Tap, CheA and/or CheW were varied (with the levels of Trg and Aer unchanged). Unless specified otherwise, we used strains lacking the enzymes required for adaptation: the methyltransferase CheR and the methylesterase CheB. In these strains receptors encoded by wild-type genes remain in the half-modified state, QEQE, where Q (glutamine) mimics methylated glutamate, and receptors engineered in other modification states remain as such. Thus, all receptor molecules in *cheR cheB* cells are either identical or are of a few defined types.

We observed a strong effect of receptor homogeneity on both the sensitivity and cooperativity of the response (Fig. 1). In cells expressing native levels of Tar and Tsr (Fig. 1a), only a fraction of the CheA activity was Tar-dependent. This activity was inhibited by addition of the non-metabolizable aspartate analogue α-methyl-

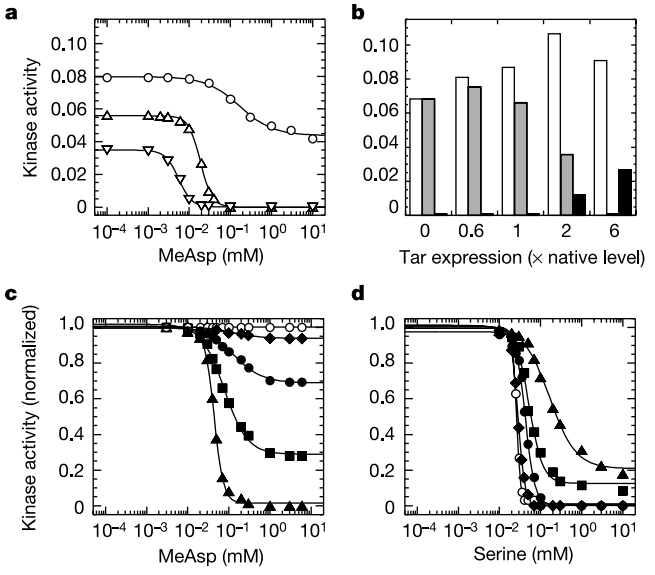


**Figure 1** Effect of the homogeneity of the receptor cluster on response to attractants. **a**, Response to MeAsp of $Tar^+$ $Tsr^+$ $Tap^+$ cells (circles), $Tar^+$ $Tap^+$ cells (triangles), or $Tar^+$ cells (inverted triangles). **b**, Effect of level of expression of Tar in $Tsr^+$ cells on the kinase activity in the absence of attractant or in the presence of a saturating dose of MeAsp (5 mM) or serine (10 mM). In all cases, a saturating dose of both attractants reduced the kinase activity to zero (not shown). White bars, no attractant; grey bars, MeASP; black bars, serine. **c**, **d**, Response of cells expressing different levels of Tar in $Tsr^+$ cells to MeAsp (**c**) or serine (**d**), normalized to the total pre-stimulus kinase activity (shown as white bars in **b**). The expression levels of Tar were 0 (open circles), 0.6 (diamonds), 1 (filled circles), 2 (squares) or 6 (triangles) times the native level. Here and in other figures kinase activity is expressed in units of FRET and solid lines are fits using the Hill equation. The fits and the best-fit values are summarized in Supplementary Information.

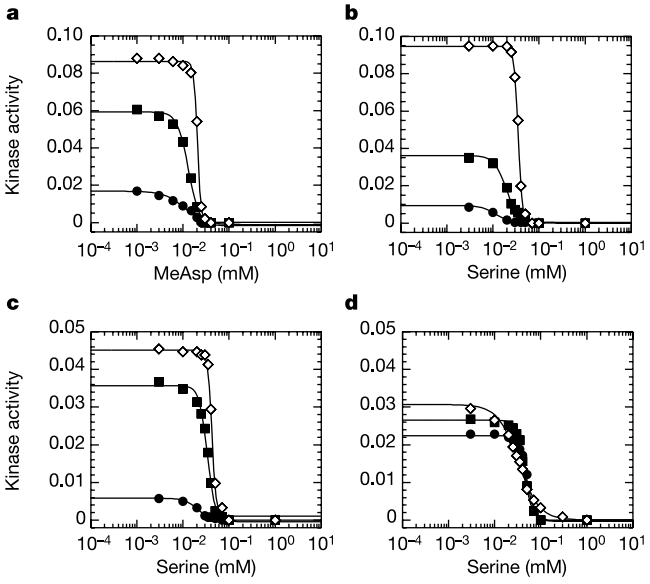


**Figure 2** Effect of the composition of the receptor–kinase complex on response to attractants. **a**, Response to MeAsp of cells expressing only Tar at 1 (filled circles), 2 (filled squares) and 6 (open diamonds) times the native level. **b**, Response to serine of cells expressing only Tsr at 0.3 (filled circles), 0.7 (filled squares) and 5 (open diamonds) times the native level. **c**, Response to serine of $Tsr^+$ cells expressing CheW at 0.01 (filled circles), 0.1 (filled squares) and 0.7 (open diamonds) times the native level. **d**, Response to serine of $Tar^+$ $Tsr^+$ $Tap^+$ cells expressing CheA at 0.25 (filled circles), 0.3 (filled squares) and 8 (open diamonds) times the native level.

aspartate (MeAsp), with a half-maximal response at $K_{1/2}$ of 160 μM. In contrast, the entire kinase activity could be inhibited by serine. Deletion of *tsr* not only made the entire CheA activity Tar-dependent, but also resulted in an approximately eightfold increase in sensitivity towards MeAsp. This increase in sensitivity was accompanied by a significant increase in the cooperativity of the response, shifting the Hill coefficient from ~1 to ~3. Additional deletion of a minor receptor, *tap*, resulted in a further roughly threefold increase in sensitivity but little change in cooperativity.

We obtained further evidence that Tar and Tsr affect each other's activity and sensitivity to attractants by varying the level of expression of Tar in a strain that was wild type for *tsr* (Fig. 1b–d). Figure 1b shows the kinase activity as a function of the level of expression of Tar before and after addition of a saturating dose of MeAsp or serine. The responses to these ligands were not additive. At low expression levels of Tar, the dominant receptor was Tsr, and the addition of serine reduced the kinase activity to zero. With Tar at six times the native level, Tar became the dominant receptor. When expression levels of Tar were increased from 0 (or 0.6) to six times the wild-type level, the sensitivity to MeAsp increased about threefold (Fig. 1c) and that to serine decreased about sixfold (Fig. 1d), whereas the Hill coefficients for the response to MeAsp increased from ~1 to ~4 (Fig. 1c) and the Hill coefficients for the response to serine decreased from ~9 to ~1 (Fig. 1d). These data suggest that receptors interact with one another in clusters—the larger the relative number of receptors of a given kind in the complex, the higher the sensitivity and cooperativity of the response to the ligand for that receptor.

We found that clusters of receptors of essentially one kind gave responses of high cooperativity, depending on the receptor to CheW to CheA ratio (Fig. 2). Increasing the level of expression of either Tar or Tsr in a *tsr tar tap* strain gave responses to MeAsp or serine with Hill coefficients increasing from ~2 to ~10, respectively (Fig. 2a, b). Similarly, increasing the level of expression of CheW in a *tar tap* strain raised the cooperativity of the response to serine, from a Hill coefficient of ~3 to ~10 (Fig. 2c). In contrast, increasing the level of expression of CheA lowered the cooperativity of the response to serine, from a Hill coefficient of ~5 to ~2 (Fig. 2d). Co-expression of both CheA and CheW at different induction levels did not affect the cooperativity of the response (data not shown).

High cooperativity was not a result of abnormally high levels of protein expression, because responses to serine with Hill coefficients

Box 1
**MWC-type models of receptor cooperativity**

The MWC model[27] can be seen as an extension of the two-state model of chemoreceptors[12–15] that includes interactions between receptors. There are two crucial assumptions: (1) the inactive state of a receptor homodimer has a higher affinity to attractant than the active state; and (2) the entire complex exists with all of its $N$ receptor homodimers either in active or inactive states. As in the two-state model, the receptor and the kinase are tightly coupled, so that the kinase is active when the receptor is active. Cooperativity of the response in this model depends not only on $N$ but on two other parameters: $L$, the ratio of the probability that the complex is in the active state to the probability that it is in the inactive state in the absence of attractant (that is, the equilibrium constant), and $c$, the ratio of dissociation constants of attractant for inactive and active states of receptors, $K_i/K_a < 1$. Panel **a** shows a complex consisting of three receptor homodimers ($N = 3$), either inactive (ovals) or active (rectangles), associated with one CheA dimer, either inactive (circle) or active (diamond). CheW, another component of the complex, is not shown. On binding of attractant (small filled triangle) to one of the receptors, the equilibrium for the entire complex shifts towards the inactive state. Because receptors in the inactive state have higher affinity to attractant, the probability that the other receptors become occupied increases, further stabilizing the inactive state. Such positive reinforcement between attractant binding and receptor inactivation results in a cooperative response to attractant. The model can be extended to any number $N$ of interacting receptor homodimers. Cooperativity (the Hill coefficient, $H$) increases with $N$ and $L$, whereas sensitivity (the inverse of the concentration at half response, $K_{1/2}^{-1}$) increases with $N$ but decreases with $L$. Panel **b** shows a simulation of the response of a receptor cluster to ligand at two values of $N$—3 (filled symbols) and 30 (open symbols)—and two values of $L$—0.3 (triangles) and $10^4$ (circles). Here $K_i = 0.03$ mM and $K_a = 1$ mM (see Supplementary Information). If $L$ is kept constant and low, the cooperativity remains approximately constant, whereas the sensitivity increases as ~$N$. Ligand binding, characterized by $K_d$ (the concentration of ligand at which half the receptors are occupied), also remains approximately constant. Panel **c** shows how values of $K_{1/2}^{-1}$, $K_d^{-1}$ and $H$ change with increasing number of interacting receptors at a constant $L = 0.3$, with values for $K_i$ and $K_a$ as in **b**.

The classical MWC model assumes that the receptor complex consists of $N$ identical subunits with the same microscopic ligand-binding affinities. In a mixed complex with the same total number of receptors but of different types, the cooperativity will be lower and will depend on the ratio between the number of different receptor species and their respective affinities to the ligand.

The assumption that the entire complex must 'flip' between the two states in a concerted fashion can be relaxed by assuming a finite coupling strength between receptors, as in the model of an extended two-dimensional receptor lattice proposed by refs 9,10. A receptor cluster of $R \approx 10^3$ receptors with a receptor complex size $N \approx 10$ can then be thought of as consisting of either $R/N$ independent all-or-none complexes or of one extended lattice in which the typical distance of signal propagation is $\sim N^{1/2}$ and the effective number of interacting receptors is $N$.

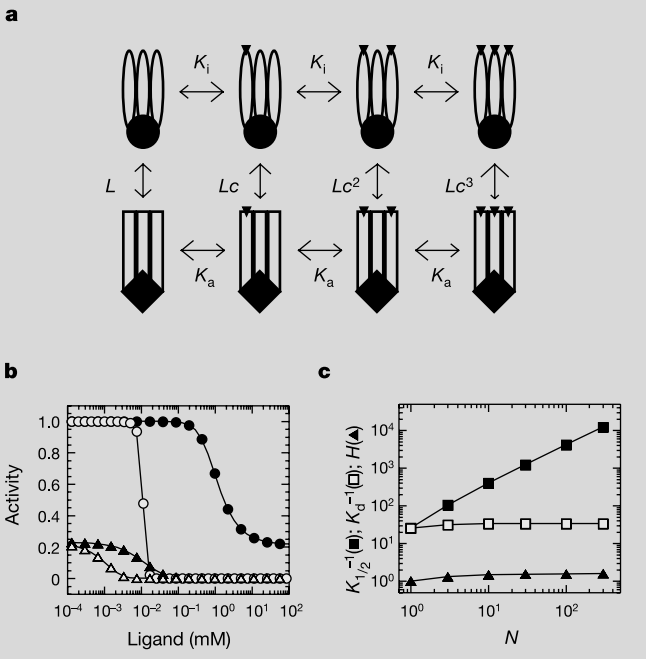

of ~10 were observed at native levels of Tsr, CheA and CheW (Figs 1d and 2c). Nor was high cooperativity an artefact due to saturation of the FRET response, because it was observed at pre-stimulus levels of 0.05–0.07, levels much lower than the highest FRET signals of 0.11 measured in our experiments (Figs 1b, d and 2c). Rather, the high cooperativity must reflect extensive interactions between receptors in native clusters. Several models have been proposed to explain the structure of receptor clusters[20,23–25]. Interest has focused on the structure consisting of two trimers of homodimers (that is, six receptor dimers) associated with one CheA dimer[20,24,26]; however, our data suggest cooperative interactions that involve more than ten receptor homodimers and thus require higher levels of organization, with a variable stoichiometry of the receptor complex.

It is possible to understand these results in the context of the classical Monod–Wyman–Changeux (MWC) model describing behaviour of multi-subunit allosteric proteins[27] (Box 1). With this model, fits to the data in both Figs 1 and 2 are virtually identical to those obtained with the Hill equation (comparisons not shown). The major effect of increasing the homogeneity of Tar on deletion of *tsr* and *tap* (Fig. 1a) is to increase the number (*N*) of interacting Tar homodimers in the complex (see Supplementary Information for parameters of the fits). In contrast, the major effect of increasing levels of expression of Tar in *tar tsr tap* cells (Fig. 2a) is to increase *L*; that is, to increase the probability that the receptor–kinase complex is in the active state in the absence of attractant. The best-fit values of *N* increased as well. Similar results were obtained for changes in levels of expression of Tsr (data not shown). Although exact best-fit values of *N* and *L* were dependent on the values assumed for dissociation constants of attractants for inactive and active receptor states (see Supplementary Information), *N* always was greater than the Hill coefficient of the fit to the same data.

Receptor interactions provide a mechanism for integrating the signal between receptors of different types, as well as between receptors in different modification states. When Tar receptors in singly modified (QEEE) and triply modified (QEQQ) states were co-expressed in the same cells, neither the initial activity nor the sensitivity to MeAsp was a simple combination of the results obtained when these receptors were expressed separately (Fig. 3a). In addition, a strain co-expressing Tsr(QEQE) with Tar(EEEE) showed lower kinase activity and was approximately 3.3 times more sensitive to serine than a strain co-expressing Tsr(QEQE) and Tar(QEQQ) (Fig. 3b). Conversely, when the activity of Tsr receptors was reduced by ~50% by the addition of serine in a strain expressing both Tsr and Tar in a QEQE state, sensitivity of Tar receptors to MeAsp increased roughly 4.5-fold (Fig. 3c). All three effects presented in Fig. 3 can be explained by analogy to the MWC model (Box 1). Receptors that are less active because they are in a low modification state and/or bound to attractant will decrease the activity and increase the sensitivity of receptors with which they interact, regardless of their type. Receptors that are more active because they are in a high modification state and/or attractant-free will have the opposite effect.

Conditions that favoured high cooperativity in *cheR cheB* cells favoured high sensitivity in wild-type ($CheR^+$ $CheB^+$) cells (Fig. 4). When expression levels of Tar were increased in wild-type cells, the sensitivity to MeAsp increased about fivefold, whereas the Hill coefficient (~2) remained unchanged (Fig. 4a). Similar results were obtained when expression levels of CheA were decreased (Fig. 4b) or when expression levels of CheW were increased (data not shown). $CheR^+$ $CheB^+$ cells have receptors with a range of modification states mixed in each receptor complex. The MWC model can be applied to mixed complexes if the ratio between inactive and active receptor states changes with receptor modification but dissociation constants of attractant for these two states remain constant[15]. Increasing levels of Tar expression in $CheR^+$ $CheB^+$ cells increases the best-fit values of *N*, whereas the values of *L* remain roughly constant (Fig. 4c). In *cheR cheB* cells, with homogeneous receptor populations, the best-fit values of *N* increase in a similar fashion, but the values of *L* increase by several orders of magnitude (Fig. 4c). Evidently, the methylation system in $CheR^+$ $CheB^+$ cells offsets this increase by adjusting the fraction of

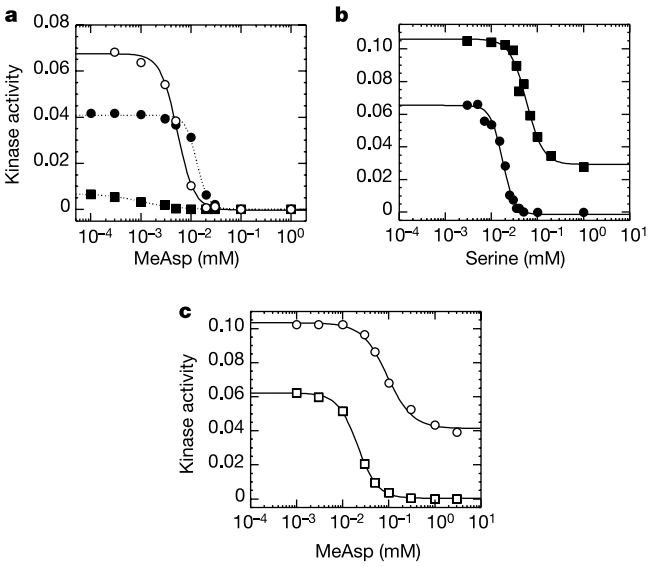


**Figure 3** Cross-talk between receptors in different modification states and between different types of receptor. **a**, Response to MeAsp of cells expressing Tar(QEEE) at ~1.5 times the native level (filled squares), Tar(QEQQ) at the native level (filled circles), or both at these levels (open circles). **b**, Response to serine of $Tsr^+$ cells expressing Tar(EEEE) (circles) or Tar(QEQQ) (squares) at ~1.5 times the native level. **c**, Response to MeAsp of $Tsr^+$ cells expressing Tar(QEQE) at ~2 times the native level, in the presence (squares) or absence (circles) of 0.07 mM serine.

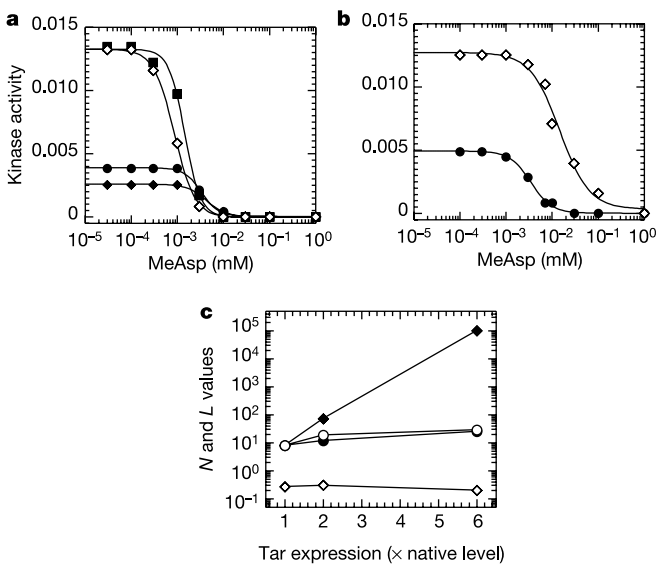


**Figure 4** Effect of complex stoichiometry on response of $CheR^+$ $CheB^+$ cells to attractant. **a**, Response to MeAsp of cells expressing only Tar at 0.6 (filled diamonds), 1 (filled circles), 2 (filled squares) and 6 (open diamonds) times the native level. **b**, Response to MeAsp of $Tar^+$ $Tsr^+$ $Tap^+$ cells expressing CheA at 0.25 (circles) and 8 (diamonds) times the native level. **c**, Best-fit values of *N* (circles) and *L* (diamonds) for fits of the MWC model to the data in Fig. 2a (filled symbols) and Fig. 4a (open symbols).

receptors in high modification states to keep the activity of the receptor complex at a moderate level (~0.3). In the MWC model, large Hill coefficients are observed only when values of both $N$ and $L$ are large, whereas high sensitivity is observed when $N$ is large and $L$ is small (Box 1). Thus, high sensitivity of wild-type cells can be explained by combination of receptor interactions and control over receptor activity. CheB is particularly crucial[22] because it generates lower modification states with lower activity and higher sensitivity. Clearly, more remains to be learned about the details of signal processing and amplification in chemotaxis, and more complicated models are required to quantitatively account for integration of signal between receptors of different types; however, the functional interactions between receptors observed here provide a framework for further experimental analysis and modelling. □

## Methods

### Plasmids

The genes *cheY–eyfp* and *cheZ–ecfp*, encoding CheY–YFP and CheZ–CFP fusions[22], were amplified with polymerase chain reaction (PCR) and cloned in tandem, using PCR-introduced *Sac*I, *Xba*I and *Hin*dIII restriction sites, into pTrc99A (AmpR, Pharmacia) under an isopropyl β-D-thiogalactoside (IPTG)-inducible promoter, yielding pVS88. All other chemotaxis proteins were expressed under the tight control of a salicylate-inducible promoter from the pLC112-derived plasmids[20]. The Tar expression plasmid pLC113, the Tsr expression plasmid pPA114, the CheA expression plasmid pPA113 and the pLC112-derived expression vector pKG110 were obtained from J. S. Parkinson. Plasmids expressing CheA and CheW or only CheW (pVS125 and pVS126, respectively) were constructed by cloning PCR-amplified *cheA* and *cheW* or *cheW* genes into *Nde*I and *Kpn*I restriction sites of pKG110. Plasmid pVS121 that expresses Tar(Q295E/Q309E) (referred to as Tar(EEEE)), pVS120 that expresses Tar(Q309E) (Tar(QEEE)) and pVS122 that expresses Tar(E491Q) (Tar(QEQQ)) were constructed by replacing the *Kpn*I/*Bam*HI fragment of pLC113 with a fragment containing corresponding mutations of *tar* that were amplified via PCR from strains VS134, VS131 and VS147 (ref. 22), respectively.

### Strains and their growth

Derivatives of *E. coli* K12 strain RP437 used in this study are listed in Supplementary Information. Ordinarily, proteins were expressed from plasmids in strains deleted for the chromosomal copy of the corresponding gene. Cells were grown as described[22] in the presence of 100 μg ml$^{-1}$ ampicillin, 34 μg ml$^{-1}$ chloramphenicol, 50 μM IPTG and varying amounts (0–1 μM) of sodium salicylate. Immunoblots, performed as before[6], were used to compare the expression levels of proteins induced by salicylate with their native expression levels. Polyclonal antibody raised against the signalling domain of Tsr[13] that reacts equally well with both Tar and Tsr was obtained from J. S. Parkinson. Polyclonal antibodies raised against CheA and CheW were obtained from R. C. Stewart.

### FRET measurements

Cells expressing CheY–YFP and CheZ–CFP were attached to a polylysine-coated coverslip and placed in a flow cell. The flow cell was kept under a constant flow (0.5 ml min$^{-1}$) of tethering buffer (10 mM potassium phosphate, 0.1 mM EDTA, 1 μM L-methionine, 10 mM sodium lactate, pH 7). Solutions of the same buffer were used to add and remove specified amounts of attractants (α-methyl-D,L-aspartate or L-serine) in a sequence of steps of increasing size. FRET, defined as the fractional change in cyan fluorescence due to energy transfer, was calculated from changes in the ratios of yellow and cyan fluorescence signals, measured as described before[22,28]. For CheR$^+$ CheB$^+$ cells, the initial response was measured (before the cells had time to adapt). A field of 300–500 cells was monitored in each experiment. Under the conditions of our experiments, interaction between CheY–YFP and CheZ–CFP provides a measure of the activity of CheA[22], so FRET data were plotted as kinase activity. Zero CheA activity was determined by adding saturating amounts of serine and MeAsp.

### Data analysis and simulations

Data analysis and simulations are described in Supplementary Information.

Received 19 November 2003; accepted 5 February 2004; doi:10.1038/nature02406.


1. Gegner, J. A., Graham, D. R., Roth, A. F. & Dahlquist, F. W. Assembly of an MCP receptor, CheW, and kinase CheA complex in the bacterial chemotaxis signal transduction pathway. *Cell* **70,** 975–982 (1992).
2. Boukhvalova, M. S., Dahlquist, F. W. & Stewart, R. C. CheW binding interactions with CheA and Tar. Importance for chemotaxis signaling in *Escherichia coli*. *J. Biol. Chem.* **277,** 22251–22259 (2002).
3. Borkovich, K. A., Kaplan, N., Hess, J. F. & Simon, M. I. Transmembrane signal transduction in bacterial chemotaxis involves ligand-dependent activation of phosphate group transfer. *Proc. Natl Acad. Sci. USA* **86,** 1208–1212 (1989).
4. Ninfa, E. G., Stock, A., Mowbray, S. & Stock, J. B. Reconstitution of the bacterial chemotaxis signal transduction system from purified components. *J. Biol. Chem.* **266,** 9764–9770 (1991).
5. Maddock, J. R. & Shapiro, L. Polar location of the chemoreceptor complex in the *Escherichia coli* cell. *Science* **259,** 1717–1723 (1993).
6. Sourjik, V. & Berg, H. C. Localization of components of the chemotaxis machinery of *Eshericia coli* using fluorescent protein fusions. *Mol. Microbiol.* **37,** 740–751 (2000).
7. Bray, D., Levin, M. D. & Morton-Firth, C. J. Receptor clustering as a cellular mechanism to control sensitivity. *Nature* **393,** 85–88 (1998).
8. Shi, Y. & Duke, T. Cooperative model of bacterial sensing. *Phys. Rev. E* **58,** 6399–6406 (1998).
9. Duke, T. A. J. & Bray, D. Heightened sensitivity of a lattice of membrane receptors. *Proc. Natl Acad. Sci. USA* **96,** 10104–10108 (1999).
10. Shimizu, T. S., Aksenov, S. V. & Bray, D. A spatially extended stochastic model of the bacterial chemotaxis signalling pathway. *J. Mol. Biol.* **329,** 291–309 (2003).
11. Mello, B. A. & Tu, Y. Quantitative modeling of sensitivity in bacterial chemotaxis: the role of coupling among different chemoreceptor species. *Proc. Natl Acad. Sci. USA* **100,** 8223–8228 (2003).
12. Asakura, S. & Honda, H. Two-state model for bacterial chemoreceptor proteins. The role of multiple methylation. *J. Mol. Biol.* **176,** 349–367 (1984).
13. Ames, P. & Parkinson, J. S. Constitutively signaling fragments of Tsr, the *Escherichia coli* serine chemoreceptor. *J. Bacteriol.* **176,** 6340–6348 (1994).
14. Barkai, N. & Leibler, S. Robustness in simple biochemical networks. *Nature* **387,** 913–917 (1997).
15. Morton-Firth, C. J., Shimizu, T. S. & Bray, D. A. Free-energy-based stochastic simulation of the Tar receptor complex. *J. Mol. Biol.* **286,** 1059–1074 (1999).
16. Borkovich, K. A., Alex, L. A. & Simon, M. I. Attenuation of sensory receptor signaling by covalent modification. *Proc. Natl Acad. Sci. USA* **89,** 6756–6760 (1992).
17. Bornhorst, J. A. & Falke, J. J. Attractant regulation of the aspartate receptor-kinase complex: Limited cooperative interactions between receptors and effects of the receptor modification state. *Biochemistry* **39,** 9486–9493 (2000).
18. Li, G. & Weis, R. M. Covalent modification regulates ligand binding to receptor complexes in the chemosensory system of *Escherichia coli*. *Cell* **100,** 357–365 (2000).
19. Gestwicki, J. E. & Kiessling, L. L. Inter-receptor communication through arrays of bacterial chemoreceptors. *Nature* **415,** 81–84 (2002).
20. Ames, P., Studdert, C. A., Reiser, R. H. & Parkinson, J. S. Collaborative signaling by mixed chemoreceptor teams in *Escherichia coli*. *Proc. Natl Acad. Sci. USA* **99,** 7060–7065 (2002).
21. Levit, M. N. & Stock, J. B. Receptor methylation controls the magnitude of stimulus–response coupling in bacterial chemotaxis. *J. Biol. Chem.* **277,** 36760–36765 (2002).
22. Sourjik, V. & Berg, H. C. Receptor sensitivity in bacterial chemotaxis. *Proc. Natl Acad. Sci. USA* **99,** 123–127 (2002).
23. Shimizu, T. S. *et al.* Molecular model of a lattice of signalling proteins involved in bacterial chemotaxis. *Nature Cell Biol.* **2,** 792–796 (2000).
24. Levit, M. N., Grebe, T. W. & Stock, J. B. Organization of the receptor–kinase signaling array that regulates *Escherichia coli* chemotaxis. *J. Biol. Chem.* **277,** 36748–36754 (2002).
25. Kim, S. H., Wang, W. & Kim, K. K. Dynamic and clustering model of bacterial chemotaxis receptors: structural basis for signaling and high sensitivity. *Proc. Natl Acad. Sci. USA* **99,** 11611–11615 (2002).
26. Kim, K. K., Yokota, H. & Kim, S. H. Four-helical-bundle structure of the cytoplasmic domain of a serine chemotaxis receptor. *Nature* **400,** 787–792 (1999).
27. Monod, J., Wyman, J. & Changeux, J.-P. On the nature of allosteric transitions: a plausible model. *J. Mol. Biol.* **12,** 88–118 (1965).
28. Sourjik, V. & Berg, H. C. Binding of the *Escherichia coli* response regulator CheY to its target measured *in vivo* by fluorescence resonance energy transfer. *Proc. Natl Acad. Sci. USA* **99,** 12669–12674 (2002).


**Supplementary Information** accompanies the paper on **www.nature.com/nature**.

**Acknowledgements** We thank J. S. Parkinson for providing some of the plasmids, strains and antibody used in this study, and R. C. Stewart for providing antibody. We also thank D. Bray, K. A. Fahrner, J. J. Falke, J. S. Parkinson, T. Shimizu and A. Vaknin for comments on the manuscript. We thank P. Zucchi for technical help. This research was supported by the NIH.

**Competing interests statement** The authors declare that they have no competing financial interests.

**Correspondence** and requests for materials should be addressed to H.C.B. (hberg@biosun.harvard.edu).

# Enzymic activation and transfer of fatty acids as acyl-adenylates in mycobacteria

**Omita A. Trivedi, Pooja Arora, Vijayalakshmi Sridharan, Rashmi Tickoo, Debasisa Mohanty & Rajesh S. Gokhale**

*National Institute of Immunology, Aruna Asaf Ali Marg, New Delhi 110 067, India*

**The metabolic repertoire in nature is augmented by generating hybrid metabolites from a limited set of gene products[1–3]. In mycobacteria, several unique complex lipids are produced by the combined action of fatty acid synthases and polyketide synthases (PKSs)[4–6], although it is not clear how the covalently sequestered**